Available online at www.sciencedirect.com
SCIENCE DIRECT®
International Journal of Pharmaceutics 251 (2003) 85–97
international journal of pharmaceutics
www.elsevier.com/locate/ijpharm

Influence of formulation parameters on gadolinium entrapment and tumor cell uptake using folate-coated nanoparticles

Moses O. Oyewumi, Russell J. Mumper *

Division of Pharmaceutical Sciences, Center for Pharmaceutical Science and Technology, College of Pharmacy, University of Kentucky, 907 Rose Street, Lexington, KY 40536-0082, USA

Received 22 July 2002; received in revised form 15 October 2002; accepted 15 October 2002

Abstract

Emulsifying wax and polyoxyl 2 stearyl ether (Brij 72) nanoparticles (2 mg/ml) containing high concentrations of gadolinium hexanedione (GdH) (0–3 mg) have been engineered from oil-in-water microemulsion templates. Solid nanoparticles were cured by cooling warm microemulsion templates (prepared at 55 °C) to room temperature in one vessel. Nanoparticles were characterized by transmission electron microscopy (TEM), photon correlation spectroscopy (PCS) and gel permeation chromatography (GPC). To obtain folate-coated nanoparticles, a folate ligand was added to either the microemulsion templates or nanoparticle suspensions at 25 °C. Since the concentration of Gd in the tumor is critical to the success of Gd-neutron capture therapy (NCT), the effects of various formulation factors on GdH entrapment in nanoparticles as well as tumor-targeting were studied. GdH entrapment in nanoparticles was affected mostly by the method of GdH incorporation and surfactant concentration used in preparing the microemulsion templates. Cell uptake studies were carried out in KB cells (human nasopharyngeal epidermal carcinoma cell line). The method of adding folate ligand to the formulations did not significantly affect nanoparticle cell uptake ($P > 0.11$; t-test). However, the concentration of folate ligand added to nanoparticles had the greatest influence on nanoparticle uptake ($P < 0.01$; t-test). The results showed that GdH entrapment and cell uptake were optimized and suggested that engineered folate-coated nanoparticles may serve as effective carrier systems for Gd-NCT of tumors.

Keywords: KB cells; Emulsifying wax; Brij 72; Surfactant; Microemulsion

1. Introduction

Site-specific delivery of drug/therapeutics is receiving increasing attention since it can lead to significant reduction in drug toxicity and increased therapeutic effects (Allen et al., 1995). Nanoparticles have been considered as effective delivery systems for many reasons including: (i) sufficient

* Corresponding author. Tel.: +1-859-257-2300x258; fax: +1-859-323-5985
E-mail address: rjmump2@uky.edu (R.J. Mumper).

0378-5173/02/$ - see front matter © 2002 Elsevier Science B.V. All rights reserved.
PII: S0378-5173(02)00587-2

physical and biological stability that may facilitate drug entrapment and controlled release (Yang et al., 1999; Maia et al., 2000) (ii) good tolerability of the components (Muller et al., 1995; Maia et al., 2000), (iii) simplicity of the formulation processing (Oyewumi and Mumper, 2002a) and (iv) possibility of scaling up the formulation process (Muller et al., 2000; Oyewumi and Mumper, 2001; Dingler and Gohla, 2002). As such, nanoparticles have been extensively employed to deliver drugs, genes, diagnostics and vaccines into specific cells/tissues of interest (Jenning et al., 2000; Coester et al., 2000; Stella et al., 2000). Recently, we demonstrated that stable nanoparticles could be engineered from oil-in-water microemulsion templates (Oyewumi and Mumper, 2001). Solid nanoparticles were cured by simply cooling the microemulsion templates (prepared at 40–60 °C) to room temperature (Oyewumi and Mumper 2001; Oyewumi and Mumper, 2002a). Apart from facilitating the production of nanoparticles having diameters less than 100 nm, the microemulsion template technique enhanced the entrapment of gadolinium acetylacetonate (GdAcAc), a poorly water soluble compound. Specifically, up to 1 mg of GdAcAc (m.p. 143 °C) was entrapped in emulsifying wax or polyoxyl 2 stearyl ether (Brij 72) nanoparticles (2 mg/ml) (Oyewumi and Mumper, 2002a).

The potential of gadolinium as an agent for neutron capture therapy (NCT) of tumors has been earlier reported (Martin et al., 1988; Barth and Soloway, 1994). Gadolinium NCT is a potential cancer therapy that utilizes a stable, non-radioactive Gd-157 nuclide delivered to tumor cells which upon irradiation by thermal or epithermal neutrons produces localized cytotoxic radiations (Barth and Soloway, 1994; Oyewumi and Mumper, 2002b). Although, Boron-10 was applied in most of the earlier NCT clinical trials (Jono et al., 1999; Mehta and Lu, 1996), many researchers have proposed gadolinium as an alternative to boron for NCT of tumors (Chen et al., 1997; Martin et al., 1988; Tokumitsu et al., 1999, 2000). The Gd-neutron capture reaction (^{157}Gd (n,γ) ^{158}Gd) emits gamma rays and Auger electrons that have long ranges in tissues (Shih and Brugger, 1992; Matsumoto, 1992; Miyamoto et al., 1999). Also the thermal neutron cross section of Gd-157 is 66 times larger than that of Boron-10. Therefore, compared with Boron-10, application of Gadolinium-157 in NCT may ensure that neutrons are absorbed more efficiently using shorter neutron irradiation times as well as to increase the probability of lethal radiation extensively hitting the target tumor. Since many Gd-based compounds are already being used as contrast agents in magnetic resonance imaging (MRI), Gd-NCT may also afford the opportunity of coordinating and achieving both diagnostic and therapeutic purposes simultaneously.

In Gd-NCT, a selective therapeutic effect can be achieved by targeting sufficient amounts of Gd-157 nuclide to the target tumor cells, which are later specifically exposed to an external neutron source. Thus, to enhance the success of Gd-NCT, Gd delivery systems are continually being sought that will localize and retain high concentrations of Gd-157 within the tumor site prior to neutron irradiation. Reports from earlier studies, showed that higher tumor regression rates after Gd-NCT can be facilitated using tumor-targeted Gd delivery systems that will ensure accumulation of high concentrations of Gd-157 at the target tumor site (Akine et al., 1990; Tokuuye et al., 2000). The feasibility of tumor-targeting via folate receptors has earlier been reported (Lee and Low, 1995). It has also been shown that folate-conjugated macromolecules can be specifically taken up by receptor-bearing tumor cells (Lee and Huang, 1996; Lee and Low, 1995). In particular, folate-targeted delivery of Gd could have great relevance in Gd-NCT since many of the human cancer cells overexpress folate receptors (Weitman et al., 1992; Wang and Low, 1998). Folic acid binds to the folate receptors at cell surfaces with very high affinity and is internalized by receptor-mediated endocytosis (Kamen and Caston, 1986; Lee and Low, 1994, 1995; Lee and Huang, 1996; Atkinson et al., 2001). Recently, we demonstrated that folate-coated Gd nanoparticles could be recognized and taken up by folate receptors on tumor cells (Oyewumi and Mumper, 2002b,c).

Folate-coated nanoparticles were engineered by adding a folate ligand to either the microemulsion templates (before curing nanoparticles) or nano-

particle suspensions (after curing nanoparticles) (Oyewumi and Mumper, 2002b,c). In the present study, folate-coated emulsifying wax or Brij 72 nanoparticles (2 mg/ml) containing various amounts of gadolinium hexanedione (GdH) were engineered from oil-in-water microemulsion templates. The synthesis and characterization of GdH have been reported (Oyewumi and Mumper, 2002b). Since the concentration of Gd in the tumor is critical to the therapeutic effectiveness of Gd-NCT, GdH makes a suitable choice having a relatively high weight percentage of Gd. Further, as compared with GdAcAc used in previous studies (Oyewumi and Mumper, 2002b), higher entrapment efficiencies of GdH in nanoparticles are expected due to its more ideal physical properties. Specifically, GdH has a lower melting point (55 °C) and increased hydrophobicity that may facilitate incorporation into the oil phase of oil-in-water microemulsion templates. Particular attention was placed on various formulation variables (such as the type of nanoparticle formulations, method of adding folate ligand to nanoparticles and the density of folate ligand coating on nanoparticles) that could enhance GdH entrapment in nanoparticles as well facilitate Gd tumor uptake. It is expected that achieving tumor-targeted delivery of high concentrations Gd may enhance the overall success of Gd-NCT.

2. Materials and methods

2.1. Materials

Emulsifying wax, polyoxyethylene 20 sorbitan monooleate (Tween 80) were obtained from Spectrum Chemicals (New Brunswick, NJ). Polyoxyl 20 stearyl ether (Brij 78) and Polyoxyl 2 stearyl ether (Brij 72) were purchased from Uniqema (Wilmington, DE). Distearoylphosphatidylethanolamine (DSPE), folic acid, polyoxyethylene-bis-amine (PEG-bis-amine, MW 3350), Sephadex G-75, Sepharose CL-4B, L-glutamine, fetal bovine serum (FBS) (heat inactivated), trypsin–EDTA and penicillin–streptomycin solution were purchased from Sigma Chemicals (St. Louis, MO). Fluorescein-DOPE and 7-nitro-benzoxadiolzol-4-amine (NBD) were purchased from Avanti Polar-Lipids (Alabaster, AL). KB cells (human nasopharyngeal epidermal carcinoma) were obtained from ATCC (Manassas, VA).

2.2. Preparation of oil-in-water microemulsion templates

Oil-in-water microemulsion templates were prepared using emulsifying wax or Brij 72 as the oil phase (matrix material). Briefly, about 2 mg of the matrix materials accurately weighed into glass vials was melted together with various amounts of GdH (0–3 mg) on a hotplate. To the melted mixture at 55 °C, various concentrations of either polyoxyl 20 stearyl ether (Brij 78; 100 mM) or Tween 80 (10% w/w) were added under magnetic stirring. Brij 78 was used to prepare emulsifying wax-based nanoparticles and Tween 80 was used to prepare Brij 72-based nanoparticles. Water (0.22 μm filtered) was added to make the final volume of 1 ml. The formation of oil-in-water microemulsion was verified by the clarity of the mixture and by photon correlation spectroscopy (PCS) using a Coulter N4 Plus Submicron Particle Sizer at 55 °C. To prevent the warm microemulsions from cooling during the microemulsion droplet size measurement, both the cuvette and the particle sizer sample holder were maintained at 55 °C.

2.3. Preparation of nanoparticles from microemulsion templates

Using appropriate microemulsion templates, nanoparticles were prepared using various methods of curing the warm oil-in-water microemulsion templates. These methods included simple cooling of warm microemulsions to room temperature, dilution of microemulsions with cold water (1:10 v/v), or cooling of the whole microemulsions in a freezer. A separate experiment was designed to investigate the effects of the method of addition of GdH on entrapment efficiency in nanoparticles. Control nanoparticles (containing no GdH) were engineered and cured from microemulsion templates. To the control nanoparticle suspensions (2

mg/ml) at 25 °C, 1 mg of GdH was added and the mixture was stirred for 3 h.

2.4. Characterization of nanoparticles

2.4.1. Photon correlation spectroscopy (PCS)

The particle sizes of cured solid nanoparticles were determined using a Coulter N4 Submicron Particle Sizer at 20 °C by scattering light at angle 90° for 180 s (Beckman Coulter Corporation, Miami, FL). Prior to the particle size measurement, the nanoparticles were diluted (1:10 v/v) with filtered water (0.22 μm filter, Nalgene International) to ensure that the light scattering signal as indicated by the particle counts per second (CPS) was within the sensitivity range of the instrument.

2.4.2. Gel permeation chromatography (GPC)

To obtain the GPC elution profiles of nanoparticles, 80 μl of nanoparticle suspensions was passed down Sephadex G-75 column (1.5 × 8 cm) using deionized water (0.22 μm filtered) as the mobile phase. The elution of nanoparticles was detected by laser light scattering CPS and the amounts of GdH in each fraction was measured by UV absorption at 282 nm (Hitachi U-2000) as well as by fluorescence spectroscopy (Hitachi F-2000) at 270 nm (excitation) and 550 nm (emission). Entrapped GdH co-eluted with nanoparticles at the void volume of the GPC column. The efficiency of GdH entrapment was calculated from the percentage of the ratio of the area under the GPC elution profile of GdH entrapped in nanoparticles and area under the total GPC elution profile.

2.4.3. Transmission electron microscopy (TEM)

The size and morphology of nanoparticles cured from microemulsion templates were observed using a Jeol Electron Microscope in the Imaging Facility Unit of the University of Kentucky. A carbon-coated 200-mesh copper specimen grid was glow-discharged for 1.5 min. One drop of nanoparticle suspension was deposited on the grid and allowed to stand for 1.5 min after which any excess fluid was removed with filter paper. The grid was later stained with one drop of 1% uranyl acetate (0.2 μm filtered) and allowed to dry for 10 min before examination under the electron microscope.

2.5. Synthesis of folate ligand

A folate ligand was synthesized by chemically linking folic acid to distearylethanolamine (DSPE) via a PEG spacer (Mw 3350). The method of Lee and Low (1995) was modified and used in the synthesis and characterization of folate-PEG-DSPE as previously reported (Oyewumi and Mumper, 2002b). Briefly, the procedure involved the synthesis of the two main components of the ligand: folate-PEG-NH_2 and *N*-succinyl DSPE. Folate-PEG-NH_2 was synthesized by reacting overnight in the dark at room temperature, 450 mg of polyoxyethylene-bis-amine with an equimolar amount of folic acid in 5 ml dimethylsulfoxide (DMSO) containing an equimolar amount of dicyclohexylcarbodiimide (DCC) and 10 μl pyridine. Folate-PEG-NH_2 was purified by centrifugation (to remove the insoluble by-product, dicylcohexylurea), dialysis (to remove DMSO and unreacted folic acid), and by gel permeation chromatography (GPC) using cellulose cation-exchange resin (to remove unreacted polyoxyethylene-bis-amine). To synthesize *N*-succinyl-DSPE, 100 mg of DSPE was reacted overnight with 1.2 molar equivalent of succinic anhydride in chloroform. The product was precipitated with cold acetone. To obtain the final product (folate-PEG-DSPE), *N*-succinyl-DSPE whose carboxyl group had been previously activated with DCC was reacted with folate-PEG-NH_2 overnight at room temperature in chloroform. The solvent was removed, and the precipitate of folate-PEG-DSPE was washed three times with cold acetone and stored at −20 °C. To obtain fluorescence labeled folate ligand, the procedure was modified appropriately by reacting NBD with succinic anhydride. The presence of NBD in the final folate ligand was detected by fluorescence spectroscopy (460 nm excitation and 534 nm emission). Characterization of folate-PEG-DSPE was carried out using the method of Lee and Low (1995) as well as by mass spectroscopy, GPC, thin layer chromatography

and infrared spectroscopy.

2.6. Addition of folate ligand to nanoparticle preparations

Using a stock aqueous solution of folate ligand (0.5 mg/ml), two methods were used to add the ligand to nanoparticle formulations. First, various amounts were added to microemulsion templates at 55 °C and the mixture was stirred for 15 min at 55 °C. The microemulsions were then cooled to room temperature under gentle stirring. The preparation was further gently stirred for 4 h at 25 °C to obtain folate-coated nanoparticles. In the second method, various amounts of folate ligand were added to nanoparticle suspension at 25 °C (after cooling the warm microemulsions). The mixture was then gently stirred for 4 h at 25 °C. The efficiency of folate ligand attachment/adsorption was assessed by GPC elution profiles using a Sepharose CL-4B column. Briefly, 80 μl of nanoparticle suspensions after folate ligand addition were passed down a Sepharose CL-4B column (1.5×8 cm) using deionized water (0.22 μm filtered) as the mobile phase. The elution of folate coated nanoparticles and free folate ligand in all the GPC fractions was detected either by UV absorption at 363 nm. In cases where fluorescent-labeled folate ligand was used, folate ligand elution was monitored by fluorescence intensity at 534 nm (emission) and 460 nm (excitation). In a separate study, the GPC elution profiles of control nanoparticles (without folate ligand) and free folate ligand were obtained using laser light scattering CPS and fluorescence spectroscopy, respectively, to serve as references for folate-coated nanoparticles. Prior to the uptake studies, the stability of folate ligand coating on nanoparticles was investigated to account for any detachment/leakage of the folate ligand from nanoparticles. Folate-coated nanoparticles were incubated at 37 °C for 150 min in phosphate buffer saline (PBS) (pH 7.4) and 10% FBS. The percentage of folate ligand lost was obtained from the difference between the initial amount of folate ligand coating and amount of folate ligand coating retained on nanoparticles at each time point.

2.7. Cell culture

Cell uptake studies were performed using KB cells, a human nasopharyngeal epidermal carcinoma cell line (ATCC, Manassas, VA). The cells were cultured in T-75 flasks at 37 °C in a humidified atmosphere containing 5% CO_2 using folic acid-free Dulbecco's modified Eagle's medium supplemented with 10% heat-inactivated FBS. The only source of folic acid in the media was due to the presence of the 10% FBS.

2.8. Nanoparticle cell uptake studies

The growth medium was aspirated from each T-75 flask and the KB cells monolayer was washed with sterile PBS (154 mM, pH 7.4). After aspirating the PBS, 1.5 ml of trypsin–EDTA was added to the flask to detach cells. The suspended cells in growth medium were centrifuged at 1500 rpm (4 °C) for 5 min. After discarding the supernatant, the cells were dispersed in a known volume of growth medium and the cells were counted using a hemocytometer. To study the uptake of nanoparticles, KB cells were seeded in 48-well plates at a density of 10^5 cells per well in complete growth medium and allowed to grow for 4 days, with the medium changed once on the second day. To study the effect of the method of folate ligand coating on nanoparticle uptake, emulsifying wax and Brij 72 nanoparticles coated with 6 and 2% w/w folate ligand, respectively, were used. A predetermined amount of folate ligand was added to either the microemulsion templates at 55 °C or nanoparticle suspensions at 25 °C. The medium in each well was replaced with nanoparticle suspensions (360 μg/ml) in growth medium and incubated for 30 min at 37 °C. In separate experiments, the effects of incubation time (0–120 min) and density of folate ligand coating (0.75–12% w/w) on nanoparticle uptake were studied. At the end of the incubation period, nanoparticle suspensions were removed from the wells and the cell monolayers were rinsed three times with cold PBS to remove nanoparticles that were not cell associated. Subsequently, cells were lysed using 1% Triton X-100 and cell associated fluorescence was measured using a fluorometer. The concentration of cell

internalized Gd was measured by fluorescence intensity of Gd at 270 nm (excitation) and 550 nm (emission) using a predetermined standard curve. In a separate study, nanoparticles prepared with fluorescein-DOPE (0.25% w/w) were used. The amount of fluorescent-labeled nanoparticles taken up by KB cells was measured by the intensity of internalized fluorescence at 521 nm (emission) with excitation at 497 nm. Additional control experiments were carried out to compare the total cell protein content of KB cells incubated with either 360 μg/ml folate-coated nanoparticles or PBS, pH 7.4. To determine the total cell protein content, 50 μl of the cell lysate from each well was used according to the Coomassie Plus assay protocol (Pierce, Rockford, IL).

3. Results and discussion

3.1. Engineering nanoparticles from microemulsion templates

The nanoparticle engineering process was based on the formation of oil-in-water microemulsions that were prepared at 55 °C, which upon cooling in one vessel resulted in production of nanoparticles. Emulsifying wax and Brij 72 were used as nanoparticle matrix materials. Brij 78 (polyoxyl 20 stearyl ether) and Tween 80 (polyoxylethylene 20 sorbitan monooleate) were used as surfactants. The amphipathic properties of the matrix materials as well as the hydrophilic–lipophilic balance (HLB) values of surfactants were considered ideal for the formation of oil-in-water microemulsion templates. Emulsifying wax is a non-ionic wax comprised of cetostearyl alcohol and a polyoxyethylene derivative of a fatty acid in a molar ratio of about 20:1, while Brij 72 is a polyoxyethylene alkyl ether of ethanol. GdH was incorporated in nanoparticles by the addition to the oil phase (matrix materials) of the microemulsion templates. GdH is a gadolinium complex, synthesized by the complexation of Gd^{3+} with 2,4-hexanedione (Oyewumi and Mumper, 2002b). Since the concentration of Gd is critical to the success of Gd-NCT, GdH makes a very suitable choice. Apart from the possibility of achieving high entrapment in nanoparticles, GdH has a relatively higher weight percentage of Gd when compared with other complexes of Gd (such as Gd-DTPA, Gd-DOTA, Gd-EDTA, etc). Emulsifying wax and Brij 72 nanoparticles (2 mg/ml) were made with 3.0 mM Brij 78 and 2.3 mM Tween 80, respectively. The choice of surfactant type and concentrations was based on results from earlier studies (Oyewumi and Mumper, 2002a). Thus, using the ternary systems: melted oil, surfactant and water, solid nanoparticles containing GdH were engineered from microemulsion templates by simply cooling the warm microemulsions prepared at 55 °C to room temperature in one vessel. Other engineering cooling methods (such as dilution with cold water or cooling the entire template in a freezer) did not offer any advantages with respect to reducing the sizes of cured nanoparticles.

3.2. Nanoparticle characterization and GdH entrapment

Fig. 1 shows the TEM micrograph of emulsifying wax nanoparticles (2 mg/ml) formulated with

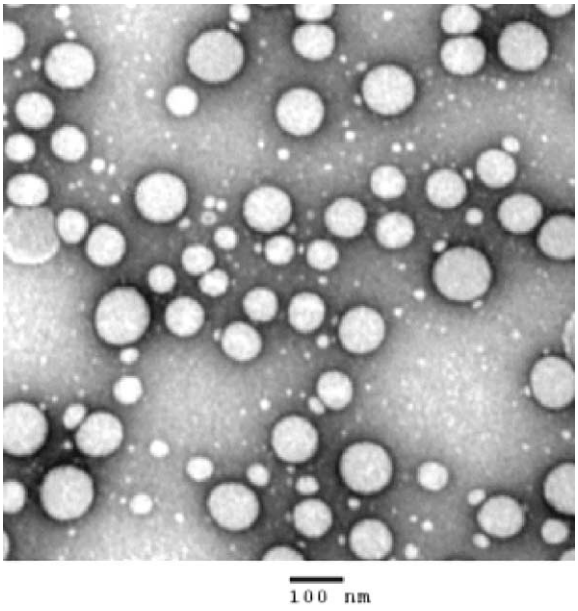

Fig. 1. Transmission electron micrograph (TEM) showing the size and morphology of emulsifying wax nanoparticles (2 mg/ml) containing 2.0 mg of GdH.

1.5 mg of GdH. It demonstrates that Gd loaded nanoparticles can be engineered directly from microemulsion templates. The nanoparticles are apparently spherical having diameters less than 100 nm (Fig. 1). Initial experiments using PCS showed that microemulsion droplet sizes at 55 °C ranged from 11±5.4 to 33±9.7 nm for both emulsifying wax and Brij 72 nanoparticle formulations. Results obtained from laser light scattering measurements of cured nanoparticles (Fig. 2) gave a similar trend as TEM results. The average particle size of emulsifying wax and Brij 72 nanoparticles (2 mg/ml) was 55±7.8 and 49±8.9 nm, respectively, and up to 3 mg of GdH could be incorporated in the nanoparticles. Importantly, the incorporation of GdH did not interfere with the nanoparticle engineering process most likely due to GdH hydrophobicity and low melting point that were compatible with the nanoparticle matrix materials. PCS measurements also showed that the polydispersity index ranged from 0.1 to 0.3 for all formulations, indicating the uniformity of particle size distribution. The GPC elution profiles in Fig. 3A demonstrate that surface adsorption or coating did not account for the entrapment of GdH in nanoparticles (Fig. 3A). As shown, only about 20% of GdH was eluted with nanoparticles when GdH was physically mixed with pre-formed emulsifying wax nanoparticles (Fig. 3A). However, the addition of GdH to nanoparticle matrix materials

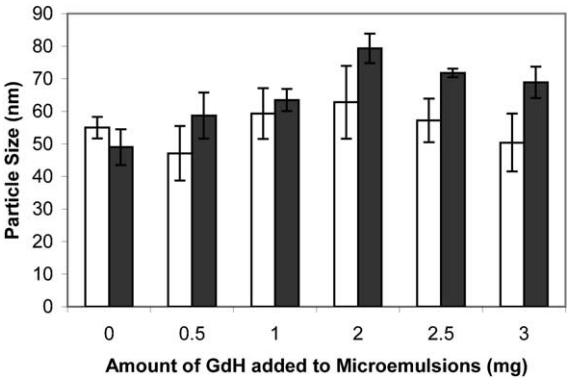

Fig. 2. Particle sizes of emulsifying wax (white bars) and Brij 72 nanoparticles (black bars) (2 mg/ml) after the incorporation of GdH (0–3 mg/ml). The particle size of each sample diluted with filtered water (1:10 v/v) was determined by laser light scattering at 25 °C. Each value represents the mean±S.D. ($n=3$).

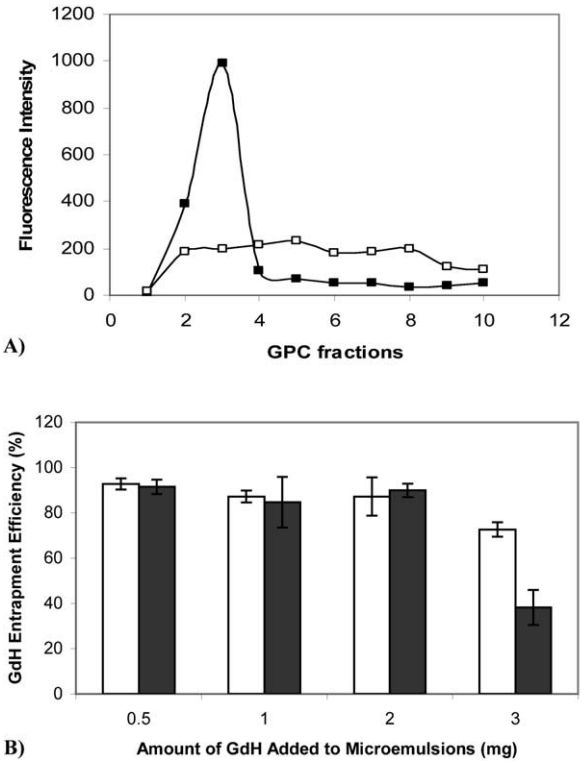

Fig. 3. (A) GPC elution profiles of GdH (1 mg/ml) entrapped (■) in emulsifying wax nanoparticles (2 mg/ml). In the control experiment, 1 mg GdH was added (□) to cured nanoparticles formulated without GdH and stirred for 3 h at room temperature. (B) The effect of GdH concentration on the entrapment efficiency in emulsifying wax nanoparticles (□) and Brij 72 nanoparticles (■) (2 mg/ml). The GPC elution profiles of free and entrapped GdH were used to calculate the entrapment efficiency. Each value represents the mean±S.D. ($n=3$).

before the formation of microemulsion templates resulted in higher entrapment efficiencies of GdH in emulsifying wax and Brij 72 nanoparticle formulations (Fig. 3A and B). The entrapment efficiencies were nearly 100% with the addition of 0.5–2 mg of GdH for both emulsifying wax and Brij 72 nanoparticles. However, using a fixed concentration of nanoparticles, GdH entrapment efficiency was reduced to about 72 and 38% in emulsifying wax and Brij 72 nanoparticles, respectively, when the GdH concentration increased to 3 mg/ml. The reduction of GdH entrapment efficiency with increase in GdH concentration could be due to surfactant micellar solubilization and/or

to a maximum solubility of GdH in the melted oil phases. The possible effect of surfactant micelles was pronounced in Brij 72 nanoparticles formulated with Tween 80. It has earlier been reported that the critical micelle concentration (CMC) of Tween 80 is 7-fold lower than that of Brij 78 (Oyewumi and Mumper, 2002a). However, at high concentrations of both Brij 78 and Tween 80, GdH entrapment efficiency was reduced. For example, GdH entrapment efficiency in emulsifying wax nanoparticles decreased from 94 to 62% by increasing Brij 78 concentrations from 3 to 12 mM (Fig. 4). A similar trend showing a decrease in GdH entrapment efficiency from 89 to 45% was observed in Brij 72 nanoparticles after increasing the Tween 80 concentration from 2.3 to 9 mM (data not shown). Therefore, the results demonstrated that GdH entrapment in nanoparticles was affected by the method of addition of GdH and surfactant (type and concentration).

3.3. Preparation and characterization of folate-coated nanoparticles

The folate ligand used in this study was synthesized to ensure folic acid linkage to DSPE via a PEG spacer (Mw 3350). The method earlier reported by Lee and Low (1995) was modified and used in the synthesis (Oyewumi and Mumper, 2002b). Previous studies showed that folate retains its receptor affinity when derivatized via its λ-carboxyl group (Lee and Low, 1995; Atkinson et al., 2001). The presence of DSPE and PEG spacer on the folate ligand is particularly expected to ensure both the attachment to nanoparticles as well as cell recognition of folate on nanoparticles. Previous studies on folate-targeted delivery systems showed that the length and flexibility of PEG spacers influenced recognition by folate receptors. Little or no cell uptake occurred in systems that contained short PEG spacers (Lee and Low, 1994; Goren et al., 2000). Since the addition of folate ligand to nanoparticles will be by physical mixing rather than covalent attachment, folate ligand adsorption/attachment onto nanoparticles was most likely facilitated by the hydrophobic groups on DSPE that served as anchors. Two methods have been used to add folate ligand to both emulsifying wax and Brij 72 nanoparticles. As described earlier, the ligand was added to either the microemulsion templates at 55 °C, (before cooling microemulsions) or to nanoparticle suspensions at 25 °C (after cooling the microemulsions). Apart from the differences in the physical nature of microemulsions and nanoparticles that could influence folate ligand attachment, a number of mechanisms may be involved in folate ligand attachment to nanoparticles such as insertion and adsorption/coating. Thus, to ensure complete folate ligand attachment to nanoparticles, sufficient time was allowed to stir the folate ligand and nanoparticle mixtures. The attachment of folate ligand to nanoparticles was verified and quantified by GPC elution profiles. The elution of folate as free folate ligand or nanoparticle associated folate ligand was measured by UV absorption of each GPC fraction at 363 nm. In cases where fluorescent-labeled folate ligand was used, the GPC elution profiles were developed by fluorescence intensity at 460 nm (excitation) and 534 nm (emission). The synthesis of fluorescent-labeled folate ligand has earlier been reported (Oyewumi and Mumper, 2002b). Using the separation of GPC elution profiles of folate as free folate ligand (alone) or nanoparticle associated folate ligand, the efficiency of folate ligand coating was obtained in all formulations. Folate ligand coating efficiency was obtained as the percentage of the ratio

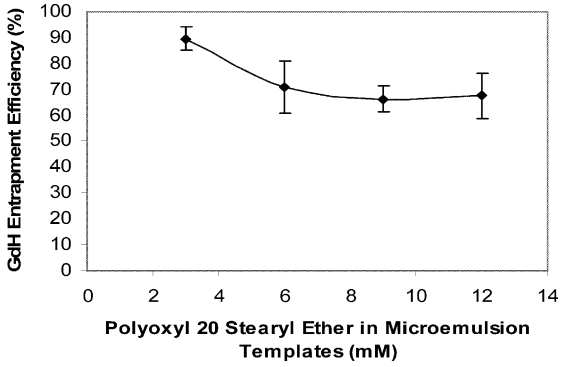

Fig. 4. The effect of polyoxyl 20 stearyl ether (Brij 78) concentration used in preparing microemulsion templates on GdH entrapment efficiency in emulsifying wax nanoparticles (2 mg/ml). The entrapment efficiency was calculated from GPC elution profiles of free and entrapped GdH. Values represent the mean ± S.D. ($n = 3$).

of the area under the folate-coated nanoparticle elution profile to the total area under the GPC folate ligand elution profile. Fig. 5 demonstrates the attachment of folate ligand to Brij 72 nanoparticles. The coating efficiencies decreased at increasing folate ligand concentration most likely due to saturation of nanoparticle surface at high folate ligand concentration (Fig. 5) For instance, for Brij 72 nanoparticles, folate ligand coating efficiency decreased from 91 to 66% when the concentration of folate ligand added to microemulsion templates increased from 0.75 to 6% w/w (Fig. 5). In most cases, the trends were comparable with folate ligand addition to either microemulsions or nanoparticle suspensions, except at high amounts of folate ligand (higher than 3% w/w), the coating efficiency was higher for the addition to nanoparticle suspensions (Fig. 5). The slightly higher coating efficiency with the addition of 3–12% w/w of folate ligand to Brij 72 nanoparticle suspensions (Fig. 5) was not significant ($P > 0.23$; t-test). Likewise, folate ligand coating efficiency of emulsifying wax nanoparticles was comparable irrespective of the method of folate ligand addition (data not shown). Particularly, folate ligand (1.5 to 12% w/w) added to either microemulsion templates or nanoparticle suspensions resulted in coating efficiencies above 90%, suggesting that slightly higher amounts of folate ligand may be coated on emulsifying nanoparticles for reasons not known.

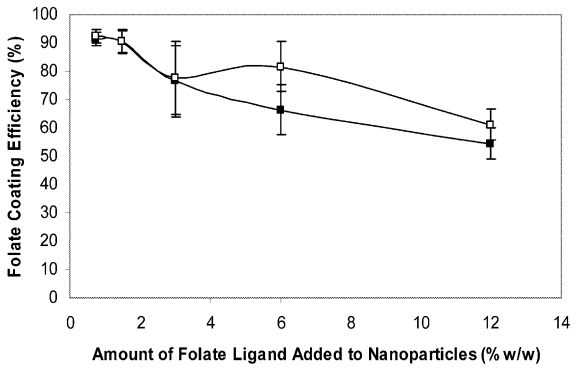

Fig. 5. The effect of concentration of folate ligand on Brij 72 nanoparticles (2 mg/ml) coating efficiency. GdH (2.0 mg) was incorporated in the nanoparticles. Folate ligand was added to either microemulsion templates at 55 °C (■) or nanoparticle suspensions at 25 °C (□). A folate ligand synthesized with a fluorescent marker was used. The fluorescence intensity of each GPC fraction was measured at 460 nm (excitation) and 534 nm (emission). Each value represents the mean ± S.D. ($n = 3$).

Since it was thought that the size of the folate-coated nanoparticles is relevant to cell uptake, further studies were carried out to investigate the effects of folate ligand coating on nanoparticle size. It was observed that the average size of folate-coated nanoparticles as determined by PCS was about 100 nm at folate ligand concentrations less than 3% w/w. However, the average nanoparticle size increased with an increase in the amount of folate ligand added. For instance, the average size (data not shown) of folate-coated emulsifying nanoparticles was 110 ± 13 nm with the addition of 12% w/w folate ligand, which was found to be significantly different from that of control nanoparticles (without folate ligand) ($P < 0.01$: t-test). Based on the reports of other researchers showing that small particles may be more efficient in targeting tumors compared with particle sizes with large sizes (Wu et al., 1993; Desai et al., 1996), it was thought that folate-coated nanoparticles having diameters of about 100 nm may be effective in achieving tumor specific delivery of Gd.

Additional experiments were carried out to investigate the stability of folate ligand coating on nanoparticles so as to account for any form of detachment or leakage of folate ligand from nanoparticles. As shown in Fig. 6, the percentage of folate ligand detached/lost from nanoparticles was only about 0.2 and 0.09% after incubation for 150 min in PBS and 10% FBS, respectively, demonstrating the stability of folate ligand coating on nanoparticles at 37 °C.

3.4. Formulation factors effects on folate-coated nanoparticles cells uptake

Cell uptake studies were carried out in KB cells (human nasopharyngeal carcinoma cell lines), since it is known that these cells over-express folate receptors (Lee and Huang, 1996). To facilitate the expression of folate receptors, the cells were cultured in medium that contained no folic acid. GdH cell uptake was monitored by fluorescence spectroscopy. Preliminary studies showed

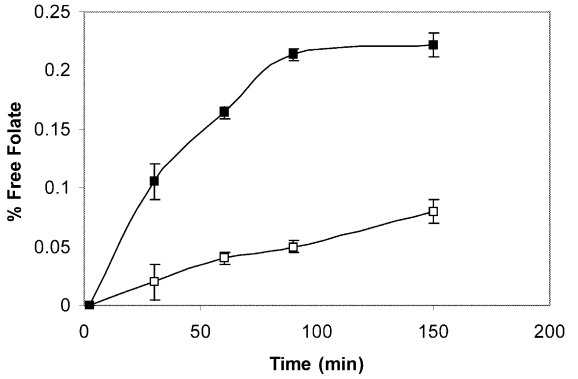

Fig. 6. Percentage of folate ligand coating that was detached from emulsifying wax nanoparticles (2 mg/ml) over time as measured by fluorescence spectroscopy using fluorescent labeled folate ligand. Folate-coated emulsifying wax nanoparticles obtained by adding folate ligand 3% w/w to nanoparticle suspensions were incubated at 37 °C with either 10 mM PBS (■) or 10% FBS (□) for 150 min. The amount of folate ligand detachment from nanoparticles was determined from GPC elution profiles of folate-coated nanoparticles at each time point. Values represent mean ± S.D. ($n = 4$).

that GdH fluorescence intensity was concentration dependent in agreement with earlier reports (Reisfeld and Biron, 1970). The standard curve of concentration versus fluorescence was linear in the concentration range of 0–50 μg/ml and the sensitivity of detection was as low as 0.1 μg/ml. Additional experiments were carried out with nanoparticles containing fluorescein-DOPE (0.25% w/w) as a fluorescence marker.

The cell uptake study was based on our earlier findings that indicated that folate-coated Gd nanoparticles can be preferentially taken up by KB cells. Folate-mediated endocytosis was demonstrated by the inhibition of folate-coated nanoparticle uptake at 4 °C as well as by the co-incubation with free folic acid. (Oyewumi and Mumper, 2002b,c). Thus, the method of folate ligand addition to nanoparticles and the density of folate ligand coating were considered as relevant to nanoparticle cell uptake. To study the effects of the method of folate ligand addition, emulsifying wax nanoparticles and Brij 72 nanoparticles coated with folate 3 and 2% w/w, respectively, were used without further purification by GPC. A predetermined amount of folate ligand was added to either the microemulsion templates at 55 °C or nanoparticle suspensions at 25 °C as earlier described. Results from cell uptake studies are shown in Fig. 7. For both emulsifying wax and Brij 72 nanoparticles, folate ligand addition to either microemulsion templates or nanoparticle suspensions resulted in comparable cell uptake ($P > 0.11$; t-test). Thus, two methods of folate ligand addition to nanoparticles were apparently equally effective. The trend could possibly be due to the expectation that folate ligand attachment to nanoparticles would occur mainly through the hydrophobic DSPE groups and less likely through the hydrophilic folic acid group. Therefore, it is conceivable that irrespective of the method of addition of to nanoparticles, folate ligand attachment will assume a similar orientation. The hydrophobic portion will most likely associate with nanoparticles with the hydrophilic portion pointing outwards towards water (continuous phase).

Additional experiments were carried out to study the effects of the density of folate ligand coating on nanoparticle uptake. Both emulsifying wax and Brij 72 nanoparticle suspensions were coated with folate ligand at concentrations ranging from 1.5 to 12% w/w and used without GPC

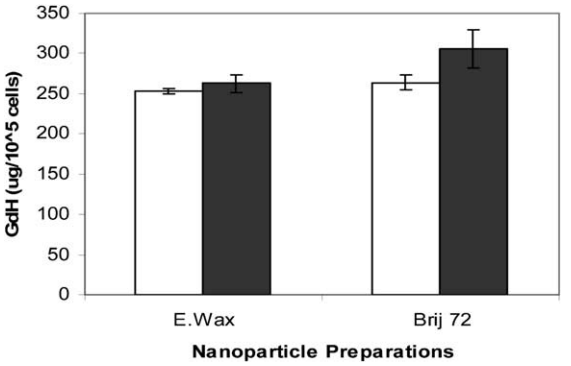

Fig. 7. The effect of the method of folate ligand addition to emulsifying wax and Brij 72 nanoparticles on KB cell uptake. Folate ligand was added either to microemulsion templates at 55 °C (□) or nanoparticle suspensions at 25 °C (■). Emulsifying wax and Brij 72 nanoparticles (2 mg/ml) were coated with 3 and 2% w/w folate ligand, respectively. After the incubation at 37 °C of folate-coated nanoparticles (360 μg/ml) with KB cells for 30 min cell internalized fluorescence was measured at 270 nm (excitation) and 550 nm (emission). Each data point represents mean of three separate experiments ± S.D.

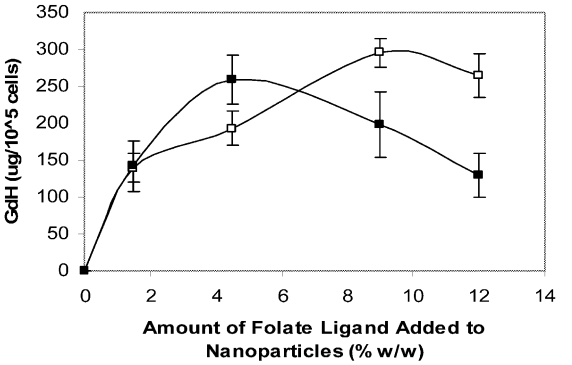

Fig. 8. The effect of the concentration of folate ligand (density of folate ligand coating) on KB cell uptake of emulsifying wax (□) and Brij 72 nanoparticles (■) (2 mg/ml). Folate-coated nanoparticles (360 μg/ml) were incubated with KB cells at 37 °C for 30 min. Cell internalized fluorescence was measured at 497 nm (excitation) and 521 nm (emission) using fluorescein-DOPE as the marker. Entrapment of fluorescein-DOPE, (0.25% w/w) in nanoparticles as confirmed by GPC was ~100%. Each data point represents the mean of three separate experiments ± S.D.

purification. As shown in Fig. 8, uptake of emulsifying wax nanoparticles increased with an increase in folate ligand concentration from 1.5 to 9% w/w ($P < 0.01$; t-test) and apparently reached a maximum between 9 and 12% w/w folate ligand concentration (Fig. 8). Also, there was an increase in Brij 72 nanoparticle uptake as folate ligand concentration increased from 1.5 to 5% w/w ($P < 0.01$; t-test), but higher concentrations of folate ligand (above 5% w/w), resulted in a decrease in Brij 72 nanoparticle uptake (Fig. 8). The reduction in nanoparticle uptake at high folate ligand concentration (above 5% w/w added to Brij 72 nanoparticles) can be attributed to the amount of free folate ligand in the nanoparticle preparations that most likely competed for binding on the receptor. As such, the results indicated that folate ligand coating facilitated nanoparticle uptake within a certain concentration range of folate ligand that resulted in little or no free folate ligand. This trend was similar to earlier studies wherein the uptake of folate-targeted delivery systems was inhibited by co-incubation with free folic acid that served as a competitive inhibitor (Lee and Low, 1995; Lee and Huang, 1996; Pan et al., 2002). A further explanation can be based on the folate ligand coating efficiency for the two nanoparticle formulations. The folate ligand coating efficiency on emulsifying wax nanoparticles was nearly 100% at folate ligand concentrations ranging from 1.5 to 9% w/w. However, for Brij 72 nanoparticles (as earlier shown in Fig. 5), the addition of folate ligand concentrations above 6% w/w resulted in ~60% coating efficiency, indicating that about 40% of folate ligand added occurred as free folate ligand.

Folate-coated nanoparticles may serve as effective carrier system for Gd-NCT for many reasons such as: (i) the nanoparticle size of ~100 nm could facilitate targeting and internalization by tumor cells (Jain, 1997), (ii) high concentration of GdH could be entrapped (iii) folate-targeted Gd delivery could potentially enhance therapeutic effectiveness of Gd-NCT. Current studies are evaluating the in vivo biodistribution of the folate-coated Gd nanoparticles using a KB cell-tumor model in athymic nude (nu/nu) mice.

4. Conclusions

Emulsifying wax and Brij 72 nanoparticles containing high concentrations of GdH have been engineered from oil-in-water microemulsions templates. Gadolinium (Gd) is a potential anticancer agent for NCT. GdH entrapment in nanoparticles was affected mostly by the method of incorporation and surfactant concentration used in preparing the microemulsion templates. Tumor targeting of nanoparticles were carried out in KB cells since they are known to over-express folate receptors. Folate-coated nanoparticles were obtained by adding a folate ligand to either the microemulsion templates at 55 °C or nanoparticle suspensions at 25 °C. Folate-targeting may have great relevance in large number of tumors that over-express folate receptors. Among the formulation variables studied, the concentration of folate added to nanoparticles had the greatest influence on nanoparticle uptake. The results showed that GdH entrapment and cell uptake were optimized and that engineered folate-coated nanoparticles may serve as effective carrier systems for Gd-NCT of tumors.

References

Akine, Y., Tokita, N., Matsumoto, T., Oyama, H., Egawa, S., Aizwa, O., 1990. Radiation effect of gadolinium-neutron capture reactions on the survival of Chinese hamster cells. Strahlenther Onkol. 166, 831–833.

Allen, T.M., Brandeis, E., Hansen, C.B., Kao, G.Y., Zaplipsky, S., 1995. A new strategy for attachment of antibodies to sterically stabilized liposomes resulting in efficient targeting to cancer cells. Biochim. Biophys. Acta 1237, 99–108.

Atkinson, S.F., Bettinger, T., Seymour, L.W., Behr, J., Ward, C., 2001. Conjugation of folate via gelonin carbohydrate residues retains ribosomal-inactivating properties of the toxin and permits targeting to folate receptor positive cells. J. Biol. Chem. 276, 27930–27935.

Barth, R.F., Soloway, A.H., 1994. Boron neutron capture therapy of primary and metastatic brain tumors. Mol. Chem. Neuropathol. 21, 139–154.

Chen, W., Mehta, S.C., Lu, R.D., 1997. Selective boron drug delivery to brain tumors for neutron capture therapy. Adv. Drug Deliv. Rev. 26, 231–247.

Coester, C.J., Langer, K., Briessen, H.V., Kreuter, J., 2000. Gelatin nanoparticles by two step desolvation—a new preparation method, surface modifications and cell uptake. J. Microencap. 17, 187–193.

Desai, M.P., Labhasetwar, V., Amidon, G.L., Levy, R.J., 1996. Gastrointestinal uptake of biodegradable microparticles in Caco-2 cells is size dependent. Pharm. Res. 14, 1568–1573.

Dingler, A., Gohla, S., 2002. Production of solid lipid nanoparticles (SLN): scaling up feasibilities. J. Microencap. 19, 11–16.

Goren, D., Horowitz, A.T., Tzemach, D., Tarshish, M.M., Zalipsky, S., Gabizon, A., 2000. Nuclear delivery of doxorubicin via folate-targeted liposomes with bypass of multidrug-resistance efflux pump. Clin. Cancer Res. 6, 1949–1957.

Jain, R.K., 1997. Delivery of molecular and cellular medicine to solid tumors. Adv. Drug Deliv. Rev. 26, 71–90.

Jenning, V., Gysler, A., Schafer-Korting, M., Gohla, S.H., 2000. Vitamin A loaded solid lipid nanoparticles for topical use: occlusive properties and drug targeting to upper skin. Eur. J. Pharm. Biopharm. 49, 211–218.

Jono, K., Ichikawa, H., Fujioka, K., Fukumori, Y., Akine, Y., Tokuuye, K., 1999. Preparation of lecithin microcapsules by a dilution method using the wuster process for intraarterial administration in gadolinium neutron capture therapy. Chem. Pharm. Bull. 47, 54–63.

Kamen, B.A., Caston, J.D., 1986. Properties of a folate binding protein (FBP) isolated from porcine kidney. Biochem. Pharmacol. 35, 2323–2329.

Lee, R.J., Low, P.S., 1994. Delivery of liposomes into cultured KB cells via folate receptor-mediated endocytosis. J. Biol. Chem. 269, 3198–3204.

Lee, R.J., Low, P.S., 1995. Folate-mediated tumor cell targeting of liposome-entrapped doxorubicin in vitro. Biochim. Biophys. Acta 1233, 134–144.

Lee, R.J., Huang, L., 1996. Folate-targeted, anionic liposome-entrapped polylysine-condensed DNA for tumor cell-specific gene transfer. J. Biol. Chem. 271, 8481–8487.

Maia, S.C., Mehnert, W., Shafer-Korting, M., 2000. Solid lipid nanoparticles as drug carriers for topical glucocorticoids. Int. J. Pharm. 165, 165–167.

Martin, R.F., D'Cunha, G., Pardee, M., Allen, B.J., 1988. Induction of double-strand breaks following neutron capture by DNA-bound 157Gd. Int. J. Radiat. Biol. 54, 205–208.

Matsumoto, T., 1992. Transport calculations of depth-dose distributions for gadolinium neutron capture therapy. Phys. Med. Biol. 37, 155–162.

Mehta, S.C., Lu, R.D., 1996. Targeted drug delivery for boron neutron capture therapy. Pharm. Res. 13, 345–351.

Miyamoto, M., Hirano, K., Ichikawa, H., Fukumori, Y., Akine, Y., Tokuuye, K., 1999. Biodistribution of gadolinium incorporated in lipid emulsions intraperitoneally administered for neutron capture therapy with tumor-bearing hamsters. Biol. Pharm. Bull. 12, 1331–1340.

Muller, R.H., Mehnert, W., Lucks, J.S., Schwartz, C., Muhlen, A., Weyhers, H., Freitas, C., Ruhl, D., 1995. Solid lipid nanoparticles (SLN)—an alternative colloidal carrier system for controlled drug delivery. Eur. J. Pharm. Biopharm. 41, 62–69.

Muller, R.H., Mader, K., Gohla, S., 2000. Solid lipid nanoparticles (SLN) for controlled drug delivery—a review of the state of the art. Eur. J. Pharm. Biopharm. 50, 161–177.

Oyewumi, M.O., Mumper, R.J., 2001. Microemulsions as templates to engineer cell specific nanoparticles. Proc. Int. Symp. Control. Rel. Bioact. Mater. 28, 7179.

Oyewumi, M.O., Mumper, R.J., 2002a. Gadolinium-loaded nanoparticles engineered from microemulsion templates. Drug Dev. Ind. Pharm. 28, 317–328.

Oyewumi, M.O., Mumper, R.J., 2002b. Engineering tumor-targeted gadolinium hexanedione nanoparticles for potential application in neutron capture therapy. Bioconjug. Chem., in press.

Oyewumi, M.O., Mumper, R.J., 2002c. Folate-coated nanoparticles designed for tumor-targeted delivery of gadolinium. Proceedings of Second International Symposium on Tumor-Targeting Delivery Systems, vol. 47, pp. 101–103.

Pan, X.O., Wang, H., Shukia, S., Sekido, M., Adams, D.M., Tjarks, W., Barth, R.F., Lee, R.J., 2002. Boron-containing folate receptor-targeted liposomes as potential delivery agents for neutron capture therapy. Bioconjug. Chem. 13, 435–442.

Reisfeld, R., Biron, E., 1970. Determination of gadolinium in sodium borate glasses. Talanta 17, 105–108.

Shih, J., Brugger, R.M., 1992. Gadolinium as a neutron capture agent. Med. Phys. 3, 733–744.

Stella, B., Arpicco, S., Peracchia, M.T., Desmaele, D., Hoebeke, J., Renoir, M., D'Angelo, J., Cattel, L., Couvreur, P., 2000. Design of folic acid-conjugated nanoparticles for drug targeting. J. Pharm. Sci. 89, 1452–1464.

Tokumitsu, H., Ichikawa, H., Fukumori, Y., 1999. Chitosan–gadopentetic acid complex nanoparticles for gadolinium neutron capture therapy of cancer: preparation by novel emulsion droplet coalescence technique and characterization. Pharm. Res. 16, 1830–1835.

Tokumitsu, H., Hiratsuka, J., Sakurai, Y., Kobayashi, T., Ichikawa, H., Fukumori, Y., 2000. Gadolinium neutron-capture therapy using novel gadopentetic acid–chitosan complex nanoparticles: in vivo growth suppression of experimental melanoma solid tumor. Cancer Lett. 150, 177–182.

Tokuuye, K., Tokita, N., Akine, Y., Nakayama, H., Sakurai, Y., Kobayashi, T., Kanda, K., 2000. Comparison of radiation effects of gadolinium and boron neutron capture reactions. Strahlenther Onkol. 176, 81.

Wang, S., Low, P.S., 1998. Folate-mediated targeting of antineoplastic drugs, imaging agents and nucleic acids to cancer cells. J. Control. Release 53, 39–48.

Weitman, S.D., Lark, R.H., Coney, L.R., Fort, D.W., Frasca, V., Zurawski, V.R., Kamen, B.A., 1992. Distribution of the folate receptor GP38 in normal and malignant cell lines and tissues. Cancer Res. 52, 3396–3401.

Wu, N.Z., Da, D., Rudoll, T.L., Needham, D., Whorton, A.R., Dewhisrt, M.W., 1993. Increased microvascular permeability contributes to preferential accumulation of stealth liposomes in tumor tissue. Cancer Res. 53, 3765–3770.

Yang, S.C., Lu, L.F., Cai, Y., Zhu, J.B., Liang, B.W., Yang, C.Z., 1999. Body distribution in mice of intravenously injected campothecin solid lipid nanoparticles and targeting effect on brain. J. Control. Release 59, 299–307.